On The Role of Environment on Tensile Response and Fracture Behavior of A High Strength Alloy Steel

Sunil Gowda[1,*], T. S. Srivatsan[2] and Anil Patnaik[1]

[1]*Department of Civil Engineering, The University of Akron, Akron, Ohio 44325, USA*

[2]*Department of Mechanical Engineering, The University of Akron, Akron, Ohio 44325, USA*

Abstract: In this paper, the influence of exposure to an aggressive environment and concomitant degradation due to corrosion on tensile properties and fracture behavior of a high strength alloy steel in the fully annealed condition is presented and discussed. Cylindrical specimens, conforming to the specifications detailed in American Society for Testing and Materials standard (ASTM E8), were prepared for purpose of this study. A test method (GMW14872), developed by General Motors (Michigan, USA), for purpose of inducing controlled corrosion on the exposed surface, using a spray technique, was used for stimulating accelerated corrosion in an environmental chamber. This was done with the intent of establishing the influence of damage resulting from an exposure to aggressive environment on short-term mechanical properties of the chosen alloy steel. The deformed and failed samples of the chosen alloy steel were examined in a scanning electron microscope with the objective of establishing the conjoint influence of severity of environment, exposure time, nature of loading and intrinsic microstructural effects on tensile response and fracture behavior.

Keywords: ASTM A572 Structural Steel, environment, degradation, corrosion, tensile properties, fracture, microstructure.

1. INTRODUCTION

Compared to other forms of steel, such as: mild steel and stainless steel, there does exist a paucity of research in the published literature on an understanding of the mechanical properties of alloy steels for the purpose of their selection and eventual use in structural applications of interest to the industries spanning: (i) civil construction, namely: buildings and bridges, (ii) marine, and (iii) surface transportation [1]. During the last four decades, i.e. since the early 1980s, high strength, low alloy steels have become known for offering acceptable to good combination of high tensile strength, adequate fracture toughness, improved weldability coupled with better performance in environments spanning a range of aggressiveness, to include both aqueous and gaseous. The production and processing, to include both primary processing and secondary processing, of the family of high strength steels has culminated from noticeable advances in both processing science and manufacturing techniques currently in use in the steel industry, especially in the domain enveloping thermo-mechanical processing (TMP). In particular, a careful control of heating and subsequent mechanical deformation processes during production of the steel can result in influencing the microstructure, such as the formation of a fine grain size.

Due in essence to their high strength and relatively low weight, structural steels find use in several applications to include the following: (a) bridge construction, (b) use as trusses, and (c) the construction of transmission towers [1-4]. However, much in conformance with the other metals belonging to the family of steels, structural steel is easily prone to degradation upon exposure to an aggressive environment. Damage due to corrosion and its concomitant influences is one of the most common problems faced by structures made from steel. The environment is normally very aggressive and/or hostile at locations along the coast line, and both in and around chemical plants, such as salt manufacturing plants where framed steel structures are exposed to corrosion chemicals. Damage and concomitant degradation due to corrosion does contribute to the following: (a) enhancing the local stress acting within the structure, (b) a change in geometric properties, (c) a gradual or progressive reduction in cross-sectional properties of the steel structure, such as section modulus or slenderness ratio [6]. It has been estimated by the NACE International; formerly the National Association for Corrosion Engineers, that damage due to corrosion is to the tune of over two-hundred billion dollars each calendar year [7, 8]. The deleterious influence of corrosion on steel structures is global. Millions of dollars are spent worldwide for the repair and rehabilitation of steel bridges, which are often exposed to aggressive environments. This makes it all the more important to understand the mechanics and mechanisms governing the corrosion behavior of

*Address correspondence to this author at the Department of Civil Engineering, The University of Akron, Akron, Ohio 44325, USA; Tel: 330-608-8355; Fax: 330-972-6027; E-mail: sg104@zips.uakron.edu

E-ISSN: 2410-4701/16 © 2016 Avanti Publishers

steels, types of corrosion and the rate of corrosion. It is apparent that the loss of section thickness (due entirely to corrosion-induced deterioration) in either the flange or web of a structural I-beam can result in a progressive loss in sectional properties, which results in a progressive reduction in the load carrying capacity of the structural member. Environment-induced corrosion-related damage has proven itself to play a significant role in the catastrophic failure of the following [9]:

(i) The silver bridge (located in Point Pleasant, West Virginia, USA) in 1967, and;

(ii) The Mianus river bridge collapse (located in the State of Connecticut, USA).

In recent years, several corrosion models have been proposed for the purpose of identifying and understanding uniform corrosion along the length of beams.

In this paper, the results of a study on the influence of an accelerated laboratory corrosion procedure on the tensile properties and resultant fracture behavior of ASTM A572, grade 50 steel are presented. A test method (GMW14872) developed by General Motors [Detroit, MI, USA], for inducing accelerated corrosion on metals was chosen. A detailed description of this spray technique is presented in the following section on "corrosion test procedure". Subsequent to the mechanical tests, the deformed and failed samples were examined in a scanning electron microscope (SEM) for the purpose of establishing a relationship between the extent and/or severity of environment-induced damage and short-term mechanical or tensile properties of the candidate alloy steel.

2. MATERIAL

ASTM A572 Grade 50 was the alloy steel chosen for this study. In recent years, its preferential selection for use in a spectrum of structural applications has resulted in its steel being termed or categorized as "structural steel". The chemical composition of this steel is provided in Table **1**. Due to noticeable amounts of carbon and manganese, this steel is often referred to as "high-carbon, low-alloy content" steel. This steel derives its strength from the formation, presence and dispersion of fine carbide particles through the microstructure [1, 3].

Presence of carbon in the alloy steel provides solid solution strengthening while concurrently enabling a noticeable increase in hardenability arising from the formation, presence and dispersion of alloy carbide particles through the microstructure. The presence of manganese assists in the formation of carbides, which contribute, either directly or indirectly, to increased strength while concurrently resisting softening during heat treatment. To a limited extent, manganese also aids in refining the grain size resulting in an end product having a fine grain size [1, 3, 10-13]. The steel was provided in the annealed condition. Annealing was done by the manufacturer of the steel at 1700^{o} C followed by slow cooling in the furnace.

Table 1: Chemical Composition of A572 Steel (in Weight Percent)

Material	C	Mn	P	S
A572	0.25	1.35	0.04	0.05

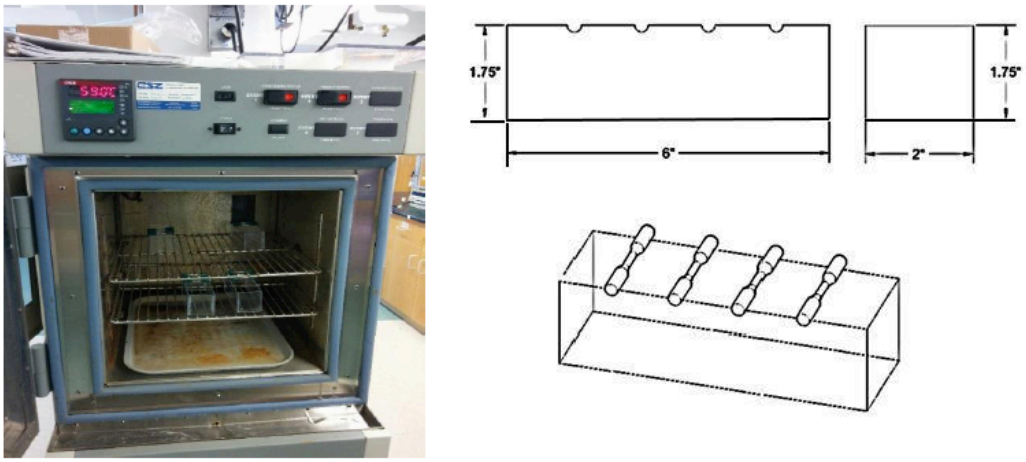

Figure 1: Environmental chamber used for retaining test specimens for specified time periods while being exposed to an aggressive aqueous environment.

3. EXPERIMENTAL PROCEDURE

3.1. The Cyclic Corrosion Laboratory Test [Categorized as GMW14872]

The chosen test procedure is an accelerated laboratory corrosion test that can be used to evaluate the corrosion properties of selected metals [14]. Concentration of the salt solution, temperature, and humidity are the three key factors that have been carefully considered to be not only important but also governing in conducting an accelerated corrosion test on metallic materials. This procedure [i.e. GMW14872] is an effective method for the purpose of evaluating different types of corrosion spanning the domains of the following: (i) general (uniform) corrosion, (ii) crevice corrosion, and (iii) galvanic corrosion. This procedure was performed, under cyclic conditions, in an environmental chamber (shown in Figure **1**) using a controlled concentration of salt solution, temperature and humidity level. The individual parameters can be varied, in an environmental chamber, so as to achieve the desired level of corrosion in a reasonable period of time. The test was run in cycles, with each cycle programmed to last for 24 hours. The required loss of material, if any, experienced by the test specimens was obtained following a specified time of exposure to the aggressive environment. In this study, the two cycles of exposure times chosen are: (i) 7 days, and (ii) 14 days.

At the end of each cycle, the specimens were thoroughly cleaned. Prior to the initiation of the next cycle, each specimen was sprayed with the salt solution, which is composed, in mass (pct.), of the following:

Sodium Chloride (NaCl):	0.9
Calcium Chloride ($CaCl_2$):	0.1
Sodium Bicarbonate ($NaHCO_3$):	0.075

The sodium chloride (NaCl) used is of the reagent type or food grade. The calcium chloride ($CaCl_2$) used was also of the reagent type and the sodium bicarbonate chosen for purpose of use was regular baking soda. The $CaCl_2$ and $NaHCO_3$ chemicals were dissolved independently in water and then added to a solution of sodium chloride.

3.2. Preparation of Test Coupon

Subsequent to exposure to the aggressive aqueous environment, the test specimens were first washed using a required amount of acetone for purpose of removing any residual paint and/or grease on the surface. This was followed by (i) rinsing in distilled water, (ii) drying using a lint-free towel, and (iii) 'light' scrubbing. Surfaces of the chosen test samples were rough polished using 600-grit silicon carbide

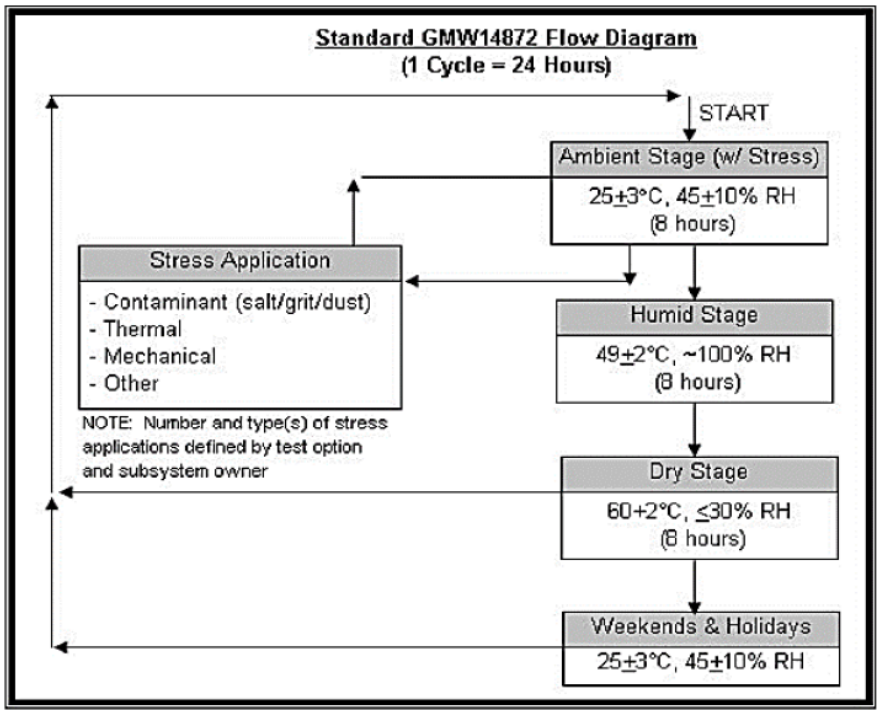

Figure 2: The flow chart depicting the accelerated corrosion procedure (GMW14872), [Ref. 18] Environmental chamber used for retaining test specimens for specified time periods while being exposed to an aggressive aqueous environment.

impregnated emery paper for purpose of removing any residual dirt that could be adhering onto the surface. Subsequent to surface preparation, the samples were: (a) labeled, (b) the thickness measured, (c) weighed, and (d) taped. It is critical that all impurities present on the surface of the alloy steel sample be completely removed prior to exposure to an aggressive environment so as to facilitate general / uniform corrosion to occur.

3.3. Preparation of Rack for the Test Coupon

The racks for holding the specimens were prepared in accordance with the dimensions shown in Figure **2**. The plates were cut from hard plexi-glass so that the material is resistant to any change in temperature and humidity that could occur in the environmental chamber during exposure. Care was taken to protect the threaded portion of the E8 samples from developing any products as a consequence of material-environment interactions, such as rust. This is essential primarily because they are tightened by screwed into the gripping part of the INSTRON servo-hydraulic test machine for performing mechanical tests. This protection was achieved by taping the threaded ends with an insulating tape.

Prior to initiation of each test; prepare test coupons were placed on the rack to monitor the test. For this particular test, two racks were used. The rack for the coupons had semicircular slots thereby ensuring that the test solution stays on the surface without having to run down, which aids in near-uniform degradation or corrosion of the metal. The exact location of each coupon on the rack was identified and recorded using pre-stamped numbers for purpose of reference.

A minimum of 5 mm spacing between the coupons and surface of the rack was maintained. All coupons were secured vertically with no more than 15-degree deviation from the vertical so as to not contact each other.

3.4. Corrosion Test Procedure

The flow diagram shown in Figure **3** describes the sequence of steps followed for testing. The cycle was repeated everyday as needed until the desired requirements for the purpose of test exposure were met. The testing was also continued on weekends so as to decrease the overall test time provided the number of cycles (N) and mass loss requirements were met.

For each salt mist application, desired spray apparatus was used to mist the samples until all areas were thoroughly wet and dripping. The quantity of spray applied was adequate to visibly rinse away any accumulation of salt left from previous sprays. The first salt mist application occurred at the beginning of the exposure. Each subsequent salt mist application was programmed to occur at approximately hour and a half following the preceding application in order to allow adequate time for the test sample to dry.

At the end of each cycle (24 hours), the coupons were: (i) removed from the testing chamber, (ii) washed with De-ionized water (DI water), (iii) sprayed with the test solution, and (iv) put back into the chamber. The

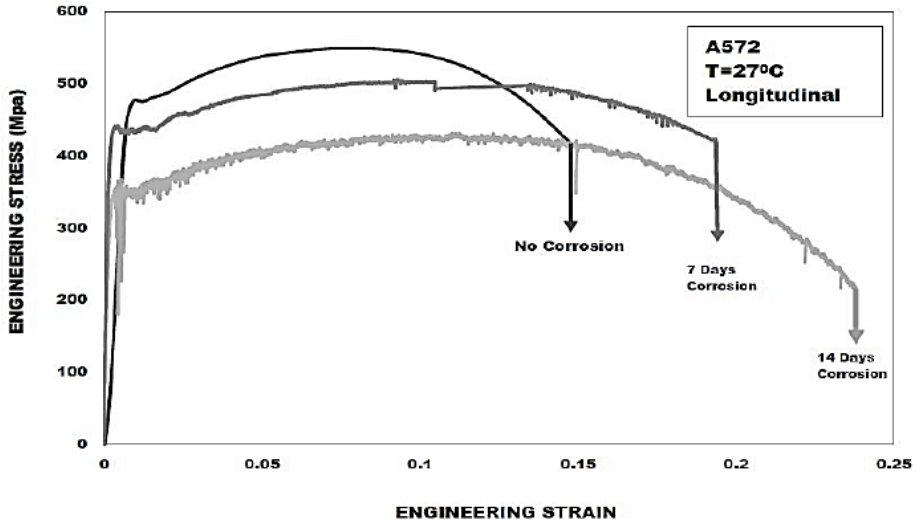

Figure 3: Influence of time of exposure to aggressive aqueous environment on engineering stress versus engineering strain response for longitudinal (L) orientation of alloy steel A572.

different stages, depicted in the flow diagram, are automatically controlled by the test chamber.

3.5. Mechanical Testing

Cylindrical test specimens, conforming to specifications detailed in ASTM E-8-10 (American Society for Testing Material, 2010) [ASTM, 2010], were precision machined from the chosen steel. The threaded test specimens measured 59 mm in length and 6.35 mm in diameter at the thread section. The gage section of the machined test specimen measured 12.5 mm in length and 3.175 mm in diameter. To minimize the effects of surface irregularities and finish, the gage sections of the machined test specimens were mechanically ground using progressively finer grades of SiC impregnated emery paper. The purpose of polishing was to remove any and all of the circumferential scratches and surface machining marks.

Uniaxial tensile tests were performed up until failure on a fully-automated, closed-loop servo-hydraulic mechanical test machine [INSTRON Model 8500 plus] equipped with a 100KN load cell. The test specimens were deformed at a constant strain rate of 0.0001/sec. An axial 12.5 mm gage length extensometer was attached to the test specimen at the gage section, using rubber bands, to provide a precise measurement of strain during uniaxial loading and resultant stretching of the test specimen. The stress and strain measurements, parallel to the load line, were recorded on a PC-based data acquisition system [DAS].

3.6. Failure-Damage Analysis

Fracture surfaces of the steel samples that were deformed and failed in uniaxial tension were carefully examined in a scanning electron microscope (SEM) to determine the macroscopic fracture mode and to concurrently characterize the fine scale topography of the tensile fracture surface that would aid in establishing the fine microscopic mechanisms governing failure during tensile loading. This is essential in an attempt to bring out the role of alloy carbides present in the microstructure of this high strength alloy steel. The macroscopic mode refers to the overall mode of failure at the 'global' level, while the microscopic mode considers any and all of the failure processes occurring at the fine microscopic or "local" level. Samples for observation in the scanning electron microscope (SEM) were obtained from the deformed and failed specimens by sectioning parallel to the fracture surface, i.e. slicing perpendicular to the major stress axis.

4. RESULTS AND DISCUSSION

4.1. Tensile Response

The tensile properties for both the longitudinal (L) and transverse (T) orientations for the chosen structural steel, for the two different exposure times, i.e. 7 days and 14 days, are summarized in Table **2**. Results reported are the mean values based on duplicate tests.

For testing in laboratory air and at the two chosen exposure times; that is, 7-day exposure and 14-day exposure, the yield strength and ultimate tensile strength was fairly consistent in both the longitudinal (L) and transverse (T) orientation. In both orientations, i.e. L and T, the tensile strength was noticeably higher than the yield strength indicating the occurrence of strain hardening beyond yield. Upon exposure for time periods of 7-days and 14-days to the aggressive aqueous environment, the yield strength and tensile strength of the chosen alloy steel revealed an

Table 2: Uniaxial Tensile Properties of Structural Steel A572 for the Two Different Exposure Times and No-Exposure

Exposure Condition	Orientation	Elastic Modulus		Yield Strength		UTS		Elongation (%)	Reduction in Area (%)
		Ksi	GPa	ksi	MPa	Ksi	MPa		
No Exposure	Longitudinal	30457	210	68	471	73	505	27	41
	Transverse	30312	209	65	447	75	516	28	41
7-Day Exposure	Longitudinal	30167	208	64	441	68	473	25	33
	Transverse	30457	210	58	405	68	474	26	33
14-Day Exposure	Longitudinal	30167	208	53	365	58	403	26	23
	Transverse	30167	208	56	387	66	459	23	23

observable decrease in comparison to values in laboratory air (27^0C).

For a fixed exposure time to the aggressive aqueous environment the elongation was fairly consistent in both the longitudinal (L) and transverse (T) orientations. Time of exposure to the aggressive aqueous environment was observed to have minimal influence on ductility, quantified by elongation over a gage length of 12.5 mm, of the chosen alloy steel. Reduction in test specimen cross-section area, another measure of ductility, was identical in both the longitudinal (L) and transverse (T) orientations, for a given exposure time to the environment. Further, the reduction in test specimen cross-section area was observed to decrease for both the longitudinal (L) and transverse (T) orientations with increased time of exposure to the aggressive aqueous environment upon comparison with values obtained from tests done in room temperature (27^0C), laboratory air environment. Influence of exposure time to the aggressive aqueous environment on engineering stress versus engineering strain response for both the longitudinal (L) and transverse (T) orientations are shown in Figure **3** and Figure **4**.

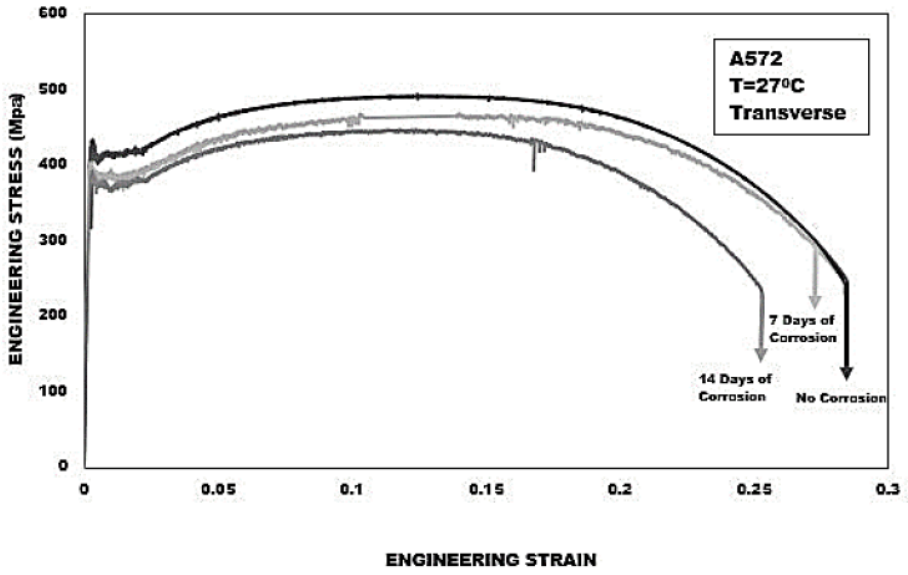

Figure 4: Influence of time of exposure to aggressive aqueous environment on engineering stress versus engineering for transverse (T) orientation of alloy steel A572.

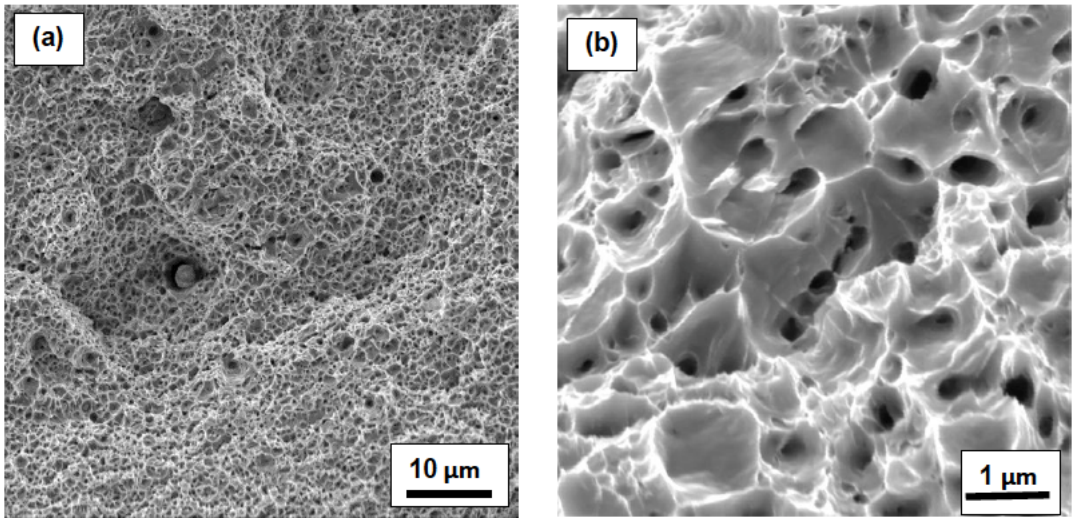

Figure 5: Scanning electron micrographs of the tensile fracture surface of non-corroded test sample of alloy steel A572 from longitudinal orientation showing. (**a**): A sizeable population of voids of varying size and shape intermingled with dimples at higher magnifications of the tensile fracture surface. (**b**): In the region of tensile overload microvoid coalescence to form fine microscopic crack.

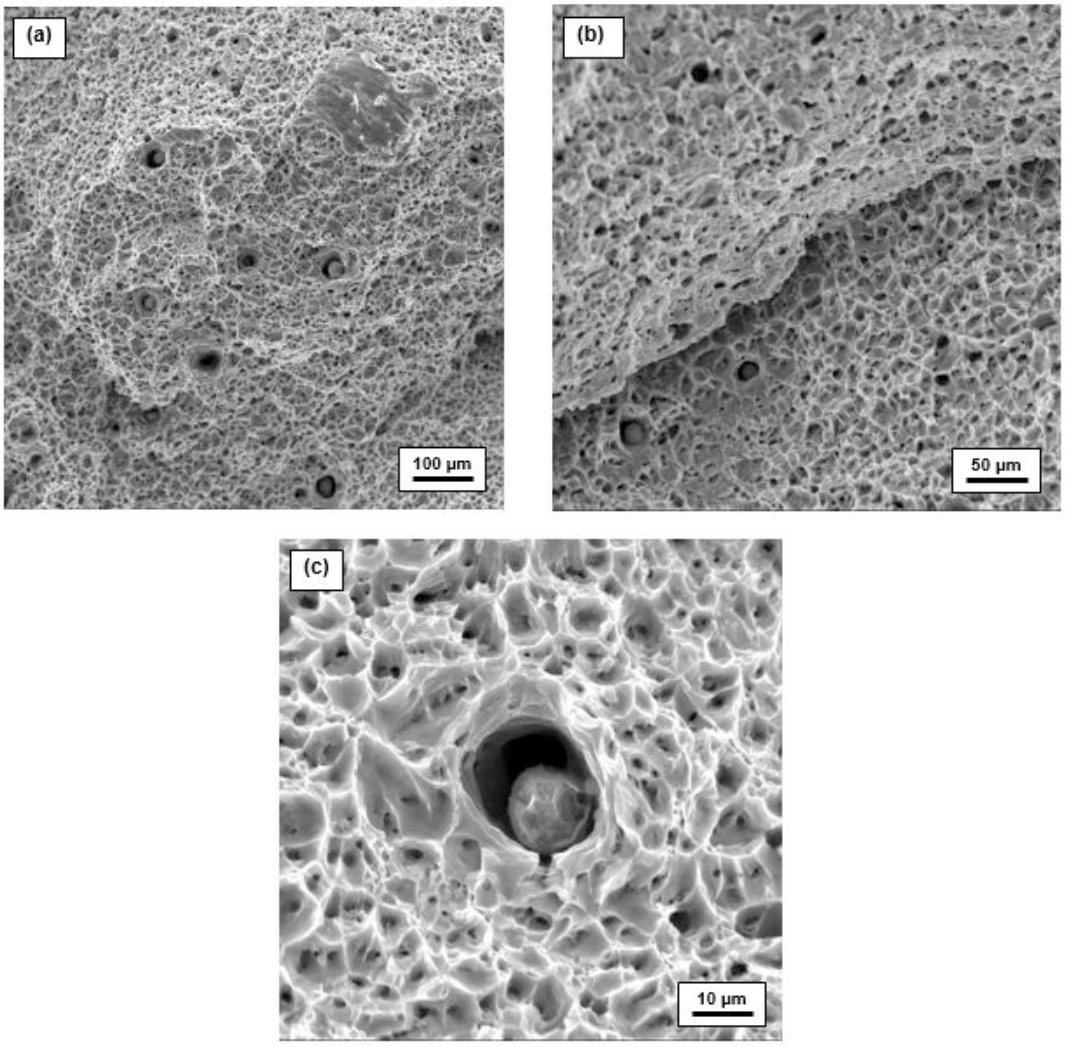

Figure 6: Scanning electron micrographs of the tensile fracture surface of transverse non-corroded sample of alloy steel A572 showing. (**a**) A sizeable population of fine microscopic voids of varying size intermingled with dimples; (**b**) Intergranular cracking in the region prior to overload; (**c**) Voids of varying size intermingled with dimples covering the overload fracture surface.

4.2. Tensile Fracture Behavior

4.2.1. As-Provided: No Exposure to Environment

In both the longitudinal (L) orientation and transverse (T) orientation scanning electron microscopy observations revealed essentially a cup-and-cone morphology indicative of globally ductile failure. High magnification observation of the fracture surface revealed isolated macroscopic cracks intermingled with voids of varying size for both the longitudinal (Figure **5a**) and transverse orientation (Figure **6a**). In fact, formation of voids surrounded by dimples of varying size and near-equiaxed shape was evident around the second-phase inclusions. These features are indicative of 'locally' operating brittle and ductile failure mechanisms. The region of overload revealed both macroscopic cracking for the case of the transverse (T) specimen (Figure **6b**) along with a sizeable population of voids of varying size along with dimples (Figure **6c**). During far-field loading, the very fine microscopic voids coalescence to form fine microscopic cracks (Figure **5b**), indicative of the occurrence of both ductile and brittle failure mechanisms at the fine microscopic level.

4.2.2. Exposure to Environment: 7 days

Following 7-day exposure to the chosen aggressive aqueous environment, both the longitudinal (L) orientation (Figure **7a**) and transverse (T) orientation (Figure **8a**) also revealed a typical cup-and-cone morphology of failure, indicative of globally ductile failure. High magnification observation of the tensile fracture surface revealed an array of fine microscopic cracks for the longitudinal (L) specimen (Figure **7b**). However, for the transverse specimen an observable population of voids of varying size and dimples were

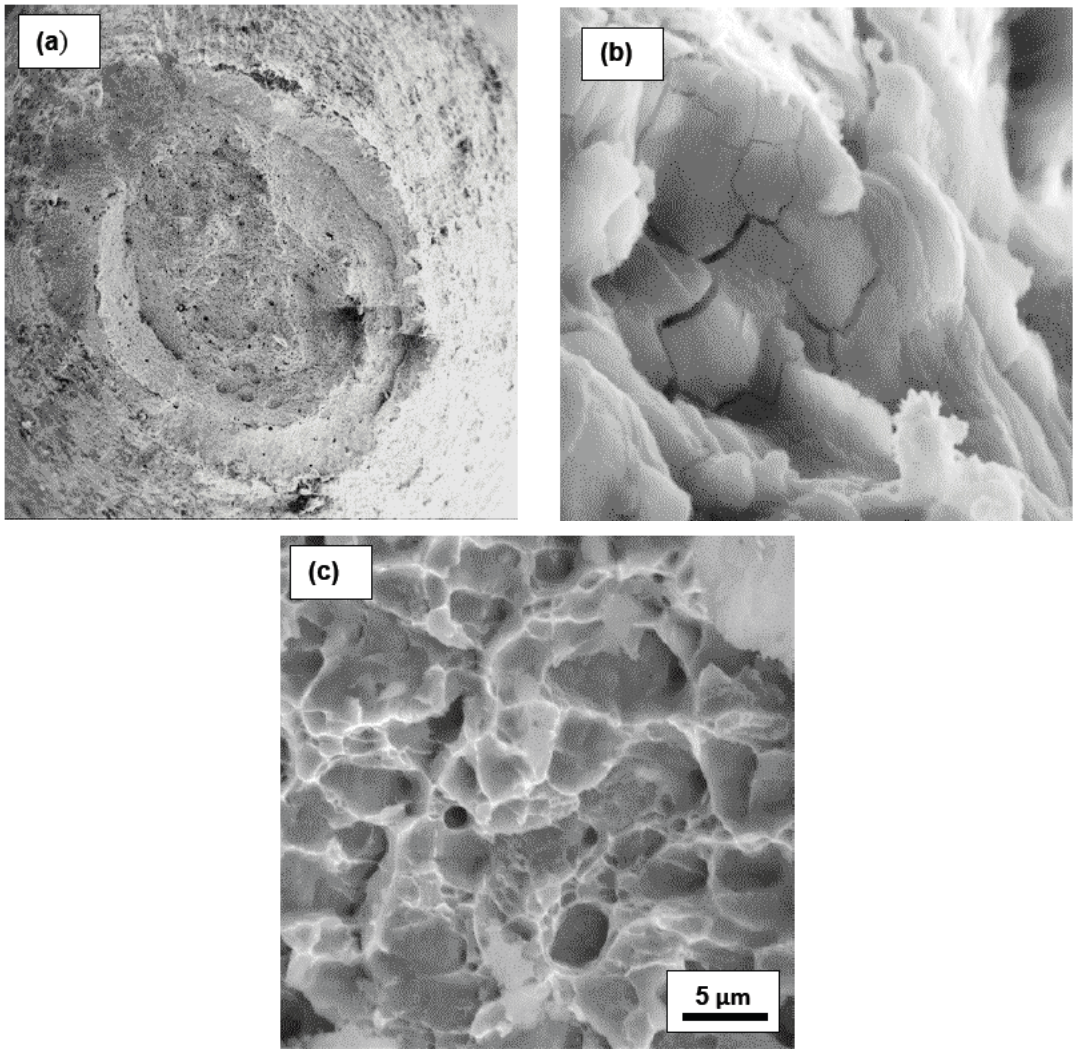

Figure 7: Scanning electron micrographs of the tensile fracture surface of sample of longitudinal orientation of alloy steel A572 exposed to 7 days to the aggressive aqueous environment and resultant degradation, showing. (**a**): Overall morphology of failure indicative of globally ductile. (**b**): High magnification observation of the region of fracture surface revealing a network of fine microscopic cracks. (**c**): Fine microscopic voids coalesce to form a microscopic crack.

distinctly observed (Figure **8b**). These fine microscopic features are indicative of "locally" operating brittle and ductile failure mechanisms. In the region approaching overload, the very fine microscopic voids coalesce to form microscopic cracks (Figure **7c**). At locations through the overload region of the transverse specimen, the voids of varying size were intermingled with cracked second-phase particles and dimples having a shear morphology indicating of the occurrence of 'local' tearing of the test specimen prior to failure (Figure **8c**).

4.2.3. Exposure to Environment: 14 Days

High magnification observation of the fracture surface of the test specimen that was exposed to the chosen aggressive aqueous environment for a time period of 14 days revealed a distinct cup-and-cone morphology. At the gradually higher allowable magnifications of the scanning electron microscope, the fracture surface revealed a healthy population of voids of varying size intermingled with fine microscopic and shallow dimples. These microscopic features are indicative of the occurrence of locally ductile failure for both the longitudinal (Figure **9a**) and transverse specimen (Figure **10a**). High magnification observation revealed a sizeable population of voids with void growth and eventual coalescence to form fine microscopic cracks (Figure **9b**) and intermingled with shallow dimples. These fine microscopic features are indicative of "locally" operating brittle and ductile failure mechanisms. The region approaching overload revealed an observable formation of fine microscopic

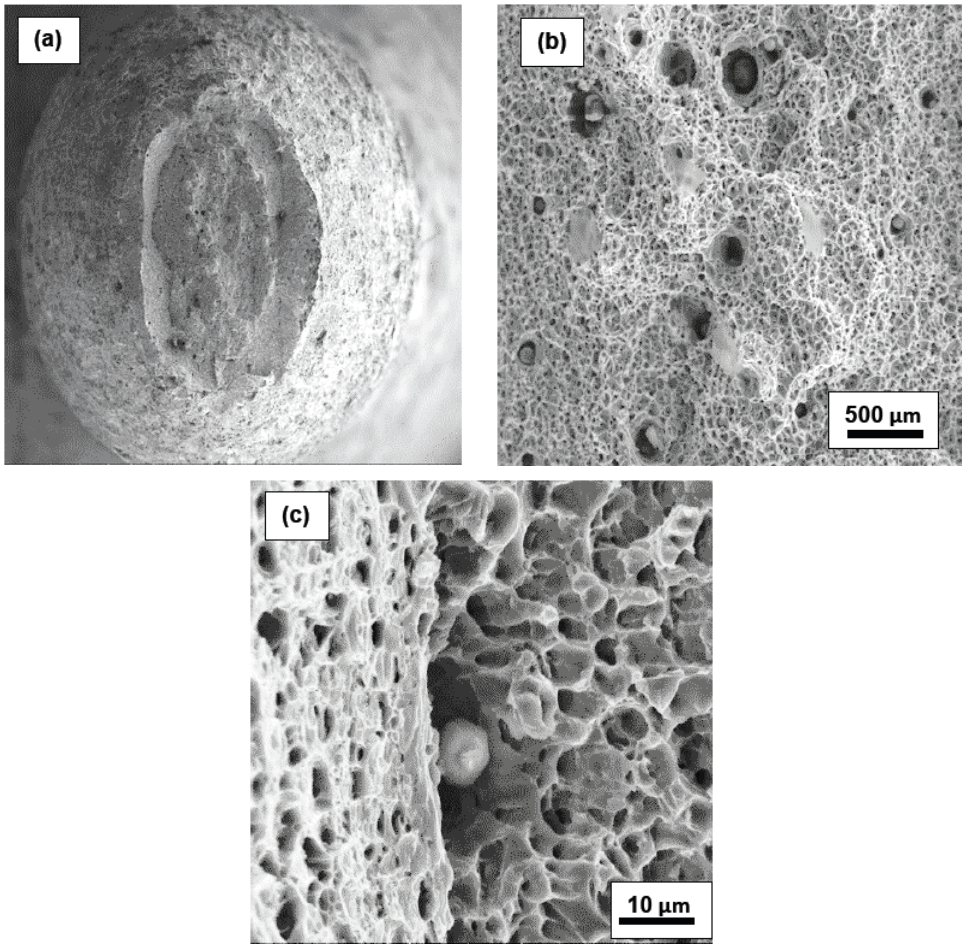

Figure 8: Scanning electron micrographs of the tensile fracture surface of sample of transverse orientation of alloy steel A572 exposed to 7 days to the aggressive aqueous environment and resultant degradation, showing. (**a**): Overall morphology of failure, cup and cone, indicate of globally ductile failure. (**b**): High magnification observation of the tensile fracture surface showing a sizeable distribution of voids of varying size intermingled with dimples, features reminiscent of locally ductile failure. (**c**): The region of overload revealing voids of varying size, cracked second-phase particles and dimples having a shear morphology.

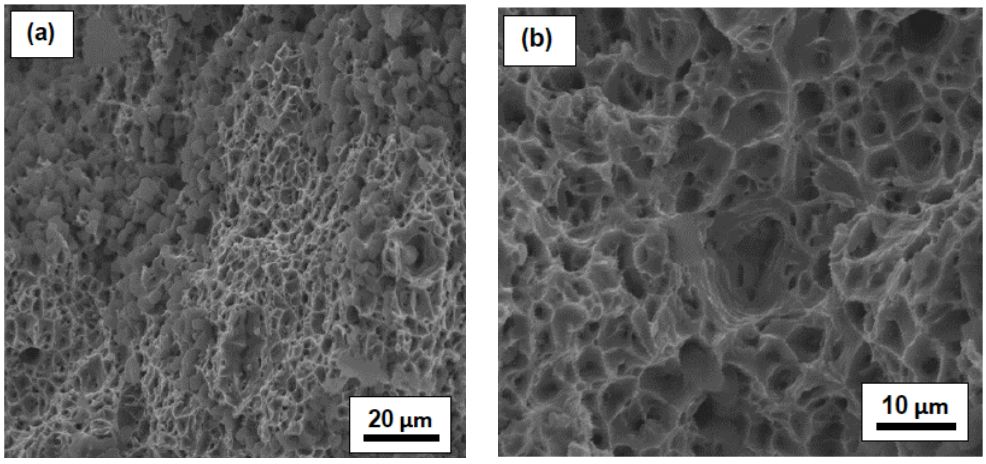

Figure 9: Scanning electron micrographs of the tensile fracture surface of longitudinal sample of A572 exposed for 14 days to the aggressive aqueous environment and resultant degradation, showing. (**a**): A sizeable population of fine microscopic voids intermingled with dimples observed on the tensile fracture surface at higher magnification. Features indicative of locally ductile failure. (**b**): High magnification observation of the region of fracture surface prior to overload revealing void growth and eventual coalescence to form fine microscopic cracks.

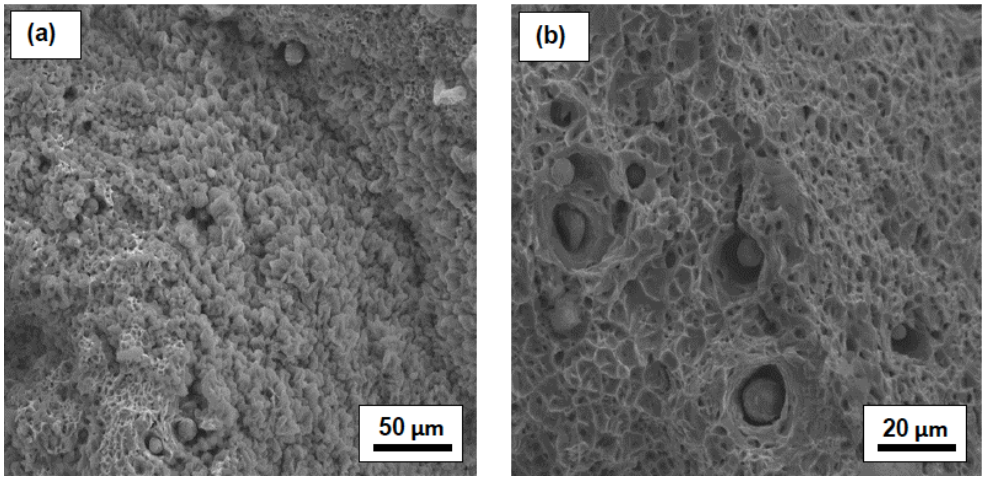

Figure 10: Scanning electron micrographs of the tensile fracture surface of transverse sample of A572 exposed for 14 days to the aggressive aqueous environmental deterioration, showing. (**a**): High magnification observation of the tensile fracture surface revealing an observable population of voids of varying size intermingled with an array of dimples. (**b**): Formation of macroscopic voids at the coarse second-phase particles distributed through the microstructure.

voids to occur at and around cracked second-phase particles. The voids of varying size were intermingled with a sizeable population of dimples (Figure **10b**).

4.3. Mechanisms Governing Load-Microstructure-Stress-Environment Interactions

During far-field loading in uniaxial tension, the coarse and intermediate size second-phase particles distributed through the microstructure of this high strength alloy steel assists in the early or premature initiation of fine microscopic voids. This is particularly favored to occur when the local strain that progressively builds up at the matrix (microstructure)-second-phase particle interface reaches a critical value and is exacerbated by material-environment interactions, which in this case is the occurrence of 'localized' corrosion of the surface at the fine microscopic level. The initiation of void at a coarse second-phase particle occurs immediately following yielding at low values of plastic strain. During far-field loading in simple tension, several of the coarse and mid-size second-phase particles either fractured or simply decohered on account of their intrinsic brittleness. This is evident by an increased level of material-environment interactions that occurs upon exposure to an aggressive environment. Continued or rapid extension of the crack is favored to occur at the prevailing high stress intensities at the 'local' level. The presence of a sizeable population of both macroscopic and fine microscopic voids is detrimental to overall ductility of this alloy steel [15, 16].

Since the voids are intrinsically softer than the hardened grains in the microstructure, the local strain is significantly elevated both at and around the region of a microscopic void enabling conditions that facilitate an increase in their volume fraction. During continued loading in the tensile stress direction the fine microscopic voids tend to gradually elongate or grow in size. The elongated voids grow and eventually coalesce by mechanisms of both void sheet formation and impingement, resulting in fine microscopic cracks [17].

CONCLUSIONS

For the as-provided alloy steel there was little to no difference in yield strength and tensile strength for both the longitudinal and transverse orientations. Further, the ductility, quantified by elongation and reduction in cross-sectional area, was identical in the two orientations.

For the longitudinal (L) orientation exposure of the alloy samples to the aggressive aqueous environment resulted in only a marginal decrease in both yield strength and ultimate tensile strength when compared to properties or strength of the as-provided, unexposed condition. Elongation did reveal minimal difference with exposure to the environment for 7 days and 14 days. There was an observable decrease in reduction in area with increased time of exposure to the aggressive aqueous environment.

For the transverse orientation both yield strength and tensile strength decreased with an increase in exposure time to the aggressive environment. The decrease in yield strength was as high as 15 percent while the decrease in tensile strength was as high as

12 percent. Increased exposure time to environment was observed to have minimal influence on elongation. With increased exposure time to the environment reduction in cross-section area revealed observable decrease when compared with the as-provided unexposed material.

For a given orientation macroscopic fracture mode was essentially cup-and-cone for both the unexposed and exposed samples, indicative of globally ductile failure. At progressively higher magnifications the fracture surface revealed a sizeable population of voids of varying size, dimples of varying shape and intermingled with isolated macroscopic and fine microscopic cracks. These features are indicative of the predominantly prevalent locally ductile failure mechanism with trace amounts of brittle failure mechanism.

ACKNOWLEDGEMENTS

This research was made possible through a research grant provided by **NCERCAMP** (The University of Akron; Program Manager: Ms. Susan Louscher) for high school students enrolled in the Summer Intern program in the College of Engineering, at The University of Akron [Akron, Ohio USA].

REFERENCES

[1] Leslie WC. The Physical Metallurgy of Steels, McGraw Hill Publishers, New York 1981; 236-246.

[2] Masahiko Fujikobo, Tetsuya Yao, Mohammad Reza Khedmati, Minoru Harada and Daisuke Yanagihara. Estimation of Ultimate Strength of Continuous Stiffened Panels Under Combined Transverse Thrust and Lateral Pressure: Part 1; Continuous Plate. Marine Structures 2005; 18; 383-410. http://dx.doi.org/10.1016/j.marstruc.2005.08.004

[3] Olson GB, Azrin M and Wright ES. Innovations in Ultra High Strength Steel Technology. Proceedings of the 34th Sagamore Army Materials Conference, U.S. Army Materials Technology Laboratory, Watertown, MA 1990; 3-65.

[4] Grondin GY, Chen Q, Elwi AE and Cheng JJ. Buckling of Stiffened Steel Plates: A Parametric Study. Journal of Constructional Steel Research 1999; 50: 151-175. http://dx.doi.org/10.1016/S0143-974X(98)00242-9

[5] ASTM E8-2010. Standard Test method for Tension Testing of Metallic Materials. American Society for Testing and Materials, ASTM, Race Street, Philadelphia, PA, 2010.

[6] Czarnecki AA and Nowak AS. Time-variant reliability profiles for steel girder bridges. Structural Safety 2008; 30(1): 49-64. http://dx.doi.org/10.1016/j.strusafe.2006.05.002

[7] Koch GH, Brongers MPH, Thompson NG, Virmani YP and Payer JH. Corrosion Cost and Preventive Strategies in the United States. Report Number FHWA-RD-01-156, Office of Infrastructure Research and Development. Federal Highway Administration, 2002.

[8] Kulicki JM, Prucz Z, Sorgenfrei DF and Mertz DR. Guidelines for evaluating Corrosion Effects in Existing Steel Bridges. National Cooperative Highway Research Program Report 333, NCHRP 1990.

[9] NSBA. Corrosion Protection of Steel Bridges. Steel Bridge Design Handbook, Chapter 23, National Steel Bridge Alliance, 2006.

[10] Metals Handbook: Properties and Selection. Classification and Designation of carbon and Low Alloy Steels. Tenth Edition, ASM International, Materials Park, Ohio, USA 1990.

[11] Bajer AJ, Laura EJ and Wei RP. Structure and Properties of Ultrahigh Strength Steels. ASTM, STP 370, American Society for Testing and Materials, Philadelphia, PA, USA 1965; 3-14.

[12] Banerjee BR. Structure and Properties of Ultrahigh Strength Steels. ASTM, STP 370, American Society for Testing and Materials, Philadelphia, PA, USA 1965; 94-109.

[13] Dieter GE. Mechanical Metallurgy, Third Edition, 1986, McGraw Hill Publishers, Boston (MA), USA, PP 410-430.

[14] General Motors Corporation. GMW14872 Cyclic Corrosion Laboratory Test. North American Engineering Standards 2006; 21 pages.

[15] Manigandan K, Srivatsan TS, Freborg AM, Quick T and Sastry S. The microstructure and mechanical properties of high strength alloy steel X2M. Advances in Materials Research 2014; 3(1): 283-2954. http://dx.doi.org/10.12989/amr.2014.3.1.283

[16] Srivatsan TS, Manigandan K and Quick T. The Impact Toughness and Fracture Behavior of Four High Strength Steels: Role of Processing. International J. of Engineering Sciences and Management 2011; 1: 2.

[17] Tvergaard V and Hutchinson JW. Material Failure by Void growth to coalescence. International Journal of Solids and Structures 2002; 39(1`3-014): 3581-3597.

Received on 18-03-2016 Accepted on 14-07-2016 Published on 13-03-2017

DOI: http://dx.doi.org/10.15377/2410-4701.2016.03.02.1

© 2016 Gowda *et al.*; Avanti Publishers.
This is an open access article licensed under the terms of the Creative Commons Attribution Non-Commercial License (http://creativecommons.org/licenses/by-nc/3.0/) which permits unrestricted, non-commercial use, distribution and reproduction in any medium, provided the work is properly cited.